



**The HEL scheme
tested with
Chemistry**

A. B. Hansen et al.

The hybrid Eulerian Lagrangian numerical scheme tested with Chemistry

**A. B. Hansen¹, B. Sørensen², P. Tarning-Andersen², J. H. Christensen¹,
J. Brandt¹, and E. Kaas²**

¹Department of Environmental Science, Aarhus University, Frederiksborgvej 399,
P.O. Box 358, 4000 Roskilde, Denmark

²Niels Bohr Institute, University of Copenhagen, Juliane Maries Vej 30,
2100 Copenhagen, Denmark

Received: 18 October 2012 – Accepted: 24 October 2012 – Published: 14 November 2012

Correspondence to: A. B. Hansen (ayobeh@umich.edu) and
B. Sørensen (sorensen@gfy.ku.dk)

Published by Copernicus Publications on behalf of the European Geosciences Union.

[Title Page](#)

[Abstract](#)

[Introduction](#)

[Conclusions](#)

[References](#)

[Tables](#)

[Figures](#)



[Back](#)

[Close](#)

[Full Screen / Esc](#)

[Printer-friendly Version](#)

[Interactive Discussion](#)



Abstract

A newly developed advection scheme, the Hybrid Eulerian Lagrangian (HEL) scheme, has been tested, including a module for atmospheric chemistry, including 58 chemical species, and compared to two other traditional advection schemes; a classical pseudospectral Eulerian method the Accurate Space Derivative (ASD) scheme and the bi-cubic semi-Lagrangian (SL) scheme using classical rotation tests. The rotation tests have been designed to test and compare the advection schemes for different spatial and temporal resolutions in different chemical conditions (rural and urban) and for different shapes (cone and slotted cylinder) giving the advection schemes different challenges with respect to relatively slow or fast chemistry and smooth or sharp gradients, respectively. In every test, error measures have been calculated and used for ranking of the advection schemes with respect to performance, i.e. lowest overall errors for all chemical species. Furthermore, the HEL and SL schemes have been compared in a shallow water model, demonstrating the performance in a more realistic non-linear deformation flow.

The results in this paper show that the new advection scheme, HEL, by far outperforms both the Eulerian and semi-Lagrangian schemes with very low error estimates compared to the two other schemes. Although no analytic solution can be obtained for the performance in the non-linear shallow water model flow, the tracer distribution appears realistic as compared to LMCSL when a mixing between local parcel concentrations is introduced in HEL.

1 Introduction

In air pollution modeling, accurate methods are important to be able to model steep gradients in the concentration fields caused by steep gradients in the emission fields and by non-linear atmospheric chemistry and non-linear atmospheric dynamics. In chemical transport models it is crucial that no negative values are generated. Not only are

GMDD

5, 3695–3732, 2012

The HEL scheme tested with Chemistry

A. B. Hansen et al.

Title Page

Abstract

Introduction

Conclusions

References

Tables

Figures



Back

Close

Full Screen / Esc

Printer-friendly Version

Interactive Discussion



they unphysical but they can also cause the chemical part of the model to break down. Negative values are generally generated when higher order transport schemes are used and special filters or limiters are therefore required to eliminate the problem.

When developing and testing new advection schemes for use in air pollution models, it is important also to consider the non-linear processes from atmospheric chemistry. In general, an advection/transport scheme should fulfill as many as possible of the desirable properties described in Rasch and Williamson (1990), Machenhauer et al. (2008), and Lauritzen and Thuburn (2011). Especially the prevention of spurious numerical mixing/unmixing, desirable property number 11 in Kaas et al. (2012), is a severe test on advection schemes, but also an essential property considering the possible amplification that the non-linear chemical schemes can induce.

Here we test the performance of a new Hybrid Eulerian Lagrangian transport scheme (HEL), Kaas et al. (2012), that has been designed to fulfill as many of the desirable properties as possible. The HEL scheme is essentially exact for non-deforming advection, and it is positive definite and monotone. For deformation flows it is important that HEL only includes so-called real mixing, i.e. no spurious unmixing takes place. Furthermore, the degree of mixing is based on the instantaneous local deformation rate of the flow, thus mimicking the effect of two-dimensional turbulence.

In Reithmeier and Sausen (2002), and later improved in Stenke et al. (2008) ATTILA (atmospheric tracer transport in a Lagrangian model) was implemented in a general circulation model to simulate transport of water vapor and cloud water. This was extended in Stenke et al. (2009) to an interactively coupled chemistry-climate model version of ATTILA, i.e. both water vapor, cloud water and mixing ratios of all chemical tracers are known for each Lagrangian parcel. ATTILA is able to maintain steep gradients, is mass conserving, and numerically non-diffusive. The ATTILA development has been a main motivator for the development of HEL. In Stenke et al. (2008) and Stenke et al. (2009), ATTILA does not handle the dry dynamics as opposed to the HEL scheme in Kaas et al. (2012) and the shallow water model part of the present work. Besides this the HEL and ATTILA approaches are quite similar when applied for non dry-dynamical prognostic

The HEL scheme tested with Chemistry

A. B. Hansen et al.

Title Page

Abstract

Introduction

Conclusions

References

Tables

Figures



Back

Close

Full Screen / Esc

Printer-friendly Version

Interactive Discussion



variables, however, ATTILA has more Lagrangian parcels per Eulerian grid cell than the version of HEL presented here, which on average only has one. More importantly, there are some differences in the way horizontal mixing between neighboring parcels are performed in ATTILA and HEL. For both schemes the degree of mixing depends on the horizontal shear deformation of the flow, however, in ATTILA this is a simple analytical expression based on Smagorinsky (1963), whereas in HEL the deformation of each parcel is kept as an additional prognostic variable, which is increased each time step in proportion to the shear deformation rate, and attempted reduced via realized mixing with neighboring parcels.

Below in Sect. 2 the HEL scheme is briefly described including a brief description of the application of chemistry in Sect. 3, this is followed by the results in Sect. 4. Section 4 is divided into subsections describing linear test cases, Sect. 4.1, ranking of error norms based on the linear test cases, Sect. 4.2, and application in a dynamical shallow water model, Sect. 4.3. The results are summarized in Sect. 5.

2 Theory

Omitting for a moment any source/sink terms and diffusion the general continuity equation for volume density reads

$$\frac{d\rho}{dt} = -\nabla \cdot (\rho \mathbf{V}), \quad (1)$$

where ρ is density and \mathbf{V} is the velocity vector. The HEL advection scheme solves Eq. (1) for all relevant chemical species. At each time step it is composed of two sets of forecasts: a set of provisional traditional forecasts represented on a fixed Eulerian grid, and a set of fully Lagrangian forecasts, i.e. forecasts represented in a field of irregularly located Lagrangian parcels.

The Eulerian represented forecast, which could be of semi-Lagrangian type, results in provisional density fields $\tilde{\rho}^{n+1}$ for the dry air density as well as for each chemical

The HEL scheme tested with Chemistry

A. B. Hansen et al.

Title Page

Abstract

Introduction

Conclusions

References

Tables

Figures

◀

▶

◀

▶

Back

Close

Full Screen / Esc

Printer-friendly Version

Interactive Discussion



species, for water vapor, and other relevant prognostic variables at the forecasted time step $n + 1$. Furthermore, for the dry air density, only, an additional forecast ρ_{adv}^{n+1} , representing the pure effect of advection is calculated, i.e. the effect of divergence can be obtained as a multiplicative factor:

$$\sigma = \frac{\tilde{\rho}^{n+1}}{\rho_{\text{adv}}^{n+1}}. \quad (2)$$

The complete Lagrangian forecast is obtained in three steps:

1. The Lagrangian parcels, each holding densities of the same prognostic variables as the Eulerian space forecast, are advected downstream from their locations at time step n to time step $n + 1$. This is a purely advective forecast in Lagrangian space.
2. The multiplicative factors from Eq. (2) are interpolated from the Eulerian grid to the location of the Lagrangian parcels at time step $n + 1$, and multiplied on all the corresponding Lagrangian densities. This is the forecast in Lagrangian space formally solving Eq. (1), i.e. without any effect of mixing between parcels. Note, that the mixing ratio for a chemical species in Lagrangian space is simply obtained by dividing its volume density with that of the dry air.
3. Since the scheme does not include any explicit diffusion a mixing of the densities between neighboring parcels is applied to the Lagrangian space forecast. This is done to mimic the effects of non-linear scale interactions. The mixing is based on the rate of deformation in the horizontal direction (only horizontal direction is considered in the present work). To avoid excessive damping the horizontal divergence is subtracted from the horizontal deformation rate when calculating the degree of mixing. This prevents damping of gravity waves when applying the method in dynamical models.

The HEL scheme tested with Chemistry

A. B. Hansen et al.

Title Page

Abstract

Introduction

Conclusions

References

Tables

Figures



Back

Close

Full Screen / Esc

Printer-friendly Version

Interactive Discussion



The HEL scheme tested with ChemistryA. B. Hansen et al.

[Title Page](#)[Abstract](#)[Introduction](#)[Conclusions](#)[References](#)[Tables](#)[Figures](#)[Back](#)[Close](#)[Full Screen / Esc](#)[Printer-friendly Version](#)[Interactive Discussion](#)

The Lagrangian forecasts are now interpolated to the Eulerian grid and used as target values toward which the provisional Eulerian forecasts are nudged. The nudging is constrained by mass conservation, monotonicity, and positive definiteness for the tracer mixing ratios. This results in the complete HEL forecast in Eulerian space. The mass conservative constraint used in the nudging ensures that the total mass in the Eulerian representation is conserved, i.e. the provisional Eulerian space forecast scheme is mass conserving, so is the corresponding HEL forecast. For details about the mixing mentioned above, the reader is referred to Kaas et al. (2012).

3 Application of chemistry in HEL

In HEL chemistry calculations are performed in Lagrangian space, i.e. for each parcel separately. The changes in mixing ratios over one dynamical time step due the chemical reactions are transferred to the Eulerian space, i.e. the regular grid, via simple bilinear interpolation weights. For Eulerian grid cells where no neighboring Lagrangian parcels are present the chemical scheme is called once again to include the effect of chemistry also here. Note, however, that this is only the case for very few – if any – Eulerian cells, so the computational burden is not affected.

4 Results

To test the newly developed scheme and compare it to existing schemes rotation tests are performed. These include the rotating cone by Molenkamp (1968) and Crowley (1968), and the slotted cylinder by Zerroukat et al. (2002). As in a previous paper, Hansen et al. (2011), results after only one rotation are considered, corresponding to one day in the chemical setup. The tests are run with different number of time steps per rotation and different number of grid points; as described in Hansen et al. (2011). In addition to showing the combined results including both advection and chemistry,

figures showing the initial condition and the individual results for chemistry and pure advection are included for comparison.

In this section selected results are shown. These are, firstly, similar figures as compared to those in the previous paper, Hansen et al. (2011), presenting a third order accurate semi-Lagrangian advection scheme (SL), and the accurate space derivatives scheme (i.e. a classical pseudospectral scheme, ASD) Frohn et al. (2002) used in the Danish Eulerian Hemispheric Model (Brandt et al., 2012), and HEL, with their respective error norms. The HEL and SL schemes are run with five different resolutions, both spatially and temporally, for varying Courant numbers. Since ASD is restricted by the CFL condition, this scheme is run with only two different resolutions, both with the same maximum Courant number. The initial conditions and setup of the test cases are described in more detail in Hansen et al. (2011).

Secondly, 6 ranking tables for the individual tests are shown along with a table ranking the 6 individual ranking tables, giving an overall rank for the study with idealized test cases.

Finally, dynamics/shallow water tests are shown, these have no reference solution. Therefore no error norms can be calculated, and the results can only be intercompared qualitatively.

4.1 Linear transport tests with chemistry

This section presents figures similar to those of Hansen et al. (2011), presenting SL, ASD, and HEL in comparison to a “reference solution” of either the initial condition or chemistry. First, results for the rotating cone considering O_3 and NO_2 for urban chemistry for the individual models are shown. These species are chosen because of they react together chemically, and their initial conditions are different. For O_3 the initial concentration is constant whereas the initial concentration of NO_2 has the shape of either the rotation cone or the slotted cylinder depending on test case. Second, the slotted cylinder is studied, showing results for pure advection, O_3 , and NO_2 for urban chemistry, in a comparison between the three schemes and the reference solution. For

The HEL scheme tested with Chemistry

A. B. Hansen et al.

Title Page

Abstract

Introduction

Conclusions

References

Tables

Figures



Back

Close

Full Screen / Esc

Printer-friendly Version

Interactive Discussion



pure advection the initial condition is used as reference solution, where as for chemistry and advection the resulting forecast after pure chemistry is used as reference solution. For each figure the corresponding l_1 , l_2 , and l_∞ error norms (see Hansen et al. (2011) for definitions) for the species in question are given.

5 In Fig. 1 results for HEL using urban chemistry and the chemical species O_3 are presented for the rotating cone with standard resolution. From visual inspection it is seen that the result is similar to that of the reference solution, also the minimum and maximum values for the reference solution and the HEL scheme are the same, namely, 50.45 and 77.47. The same can be seen from the low error measures, l_1 , l_2 , and l_∞ which are 3.7×10^{-7} , 8.5×10^{-6} , and 1.3×10^{-4} , respectively.

10 Figure 2 shows, as above, HEL using urban chemistry the rotating cone with standard resolution, but for NO_2 . As above, visually the shapes are identical, which is also in this case confirmed by minimum and maximum values that are identical and by the very low error norms. For advection the l_1 , l_2 , and l_∞ error norms are 1.6×10^{-6} , 2.4×10^{-5} , and 1.0×10^{-4} , respectively. For the solution involving urban chemistry these values are, again for l_1 , l_2 , and l_∞ , 6.3×10^{-7} , 3.8×10^{-6} , and 8.5×10^{-6} , respectively.

15 When considering the ASD scheme using urban chemistry for O_3 in the same setup as above, shown in Fig. 3, the results change, visibly the shape of the concentration changes, which is also shown in the extreme values. Both the minimum and maximum values for ASD are lower than the reference solution, 49.21 vs. 50.45 and 74.22 vs. 77.47. The l_1 , l_2 , and l_∞ error norms are 5.7×10^{-3} , 1.9×10^{-2} , and 1.4×10^{-1} , respectively.

20 Figure 4 shows ASD using urban chemistry as above, but for the chemical species NO_2 . Again, the scheme dampens and creates undershoots, however small. For pure advection, the minimum and maximum values are 0.4615 vs. 0.5 and 9.854 vs. 10, respectively, and for chemistry and advection combined the values are 0.0633 vs. 0.1369 and 10.29 vs. 11.8. For the advection, the l_1 , l_2 , and l_∞ error norms are 2.0×10^{-3} , 4.0×10^{-3} , and 1.5×10^{-2} , respectively, and for chemistry and advection combined the values for l_1 , l_2 , and l_∞ are 7.3×10^{-2} , 9.8×10^{-2} , and 1.9×10^{-1} , respectively.

The HEL scheme tested with Chemistry

A. B. Hansen et al.

[Title Page](#)[Abstract](#)[Introduction](#)[Conclusions](#)[References](#)[Tables](#)[Figures](#)[Back](#)[Close](#)[Full Screen / Esc](#)[Printer-friendly Version](#)[Interactive Discussion](#)

The HEL scheme tested with Chemistry

A. B. Hansen et al.

Title Page

Abstract

Introduction

Conclusions

References

Tables

Figures

⏪

⏩

◀

▶

Back

Close

Full Screen / Esc

Printer-friendly Version

Interactive Discussion



Results for the SL scheme using urban chemistry for O_3 are shown in Fig. 5, it is seen that the scheme smoothes the solution and dampens more than the ASD scheme. As can be seen from the extreme values the undershoots are also larger, i.e. 46.22 vs. 50.45 and 71.86 vs. 77.47. This is also evident from the error measures l_1 , l_2 , and l_∞ which are 8.2×10^{-3} , 2.7×10^{-2} , and 1.4×10^{-1} , respectively.

Figure 6 presents results for the SL scheme considering NO_2 . It is obvious that the top of the cone is smoothed by the numerical scheme both in the case of pure advection and when including chemistry. Again the minimum and maximum values are lower than those for ASD. Compared to the reference solution for pure advection the values are 0.4029 vs. 0.5 and 8.753 vs. 10, respectively. For chemistry and advection the minimum and maximum values are 0.0429 vs. 0.1369 and 10.75 vs. 11.8, respectively. The l_1 , l_2 , and l_∞ error norms for pure advection are 1.9×10^{-2} , 4.1×10^{-2} , and 1.2×10^{-1} , respectively; and 3.9×10^{-2} , 4.6×10^{-2} , and 8.9×10^{-2} , respectively, for advection and chemistry.

The following three figures present results obtained using the slotted cylinder and resolution 1_1. For each plot the results are given for reference solution (top left) and SL (top right), ASD (bottom left), and HEL (bottom right).

Figure 7 shows results for rotation test with the slotted cylinder for pure advection. The sharp gradients of the slotted cylinder is more difficult to simulate and therefore the errors increases in most of the numerical schemes. The results are for pure advection, hence no filters are added to the ASD and SL schemes, the Bartnicki filter is only applied in case of chemistry, which can also be seen from the extreme values, from top left to bottom right the minimum and maximum values are 0.5, -0.0676 , -0.0779 , and 0.5; and 10, 11.39, 11.64, and 10, respectively. The SL scheme produces the smallest over and undershoots, and gives a very smooth solution, whereas the ASD to some degree maintains the steep gradients, but also creates undershoots, the HEL scheme reproduces the shape of the slotted cylinder perfectly. The error measures for the three advection schemes are given below.

For SL the l_1 , l_2 , and l_∞ error norms are 2.1×10^{-1} , 3.1×10^{-1} , and 6.9×10^{-1} , respectively. For ASD the l_1 , l_2 , and l_∞ are 8.2×10^{-2} , 9.8×10^{-2} , and 5.6×10^{-1} , respectively. Last, for HEL the l_1 , l_2 , and l_∞ error norms are 2.0×10^{-5} , 7.0×10^{-5} , and 3.0×10^{-4} , respectively.

Figure 8 show results for the rotation test with the slotted cylinder for NO_2 for advection and chemistry combined for the three solutions for urban chemical conditions. As above the HEL scheme reproduces shape and values of the slotted cylinder perfectly, SL smoothes the result, and ASD creates massive overshoots. The minimum and maximum values are, again top left to bottom right, 0.1369, 0.0000, 0.0000, and 0.1369 and 11.80, 16.42, 269.2, and 11.80, respectively. The l_1 , l_2 , and l_∞ error norms for SL, ASD, and HEL are 5.1×10^{-1} , 5.7×10^{-1} , and 1.2×10^0 ; and 1.0×10^1 , 1.0×10^1 , and 2.2×10^1 ; and 1.7×10^{-5} , 5.2×10^{-5} , and 2.2×10^{-4} , respectively.

The final figure of this section, Fig. 9, presents the slotted cylinder as above, but here the results for O_3 are shown. The most significant difference compared to the two plots above is that for ASD the shape of the slotted cylinder now is completely “inverted”, i.e., the cylinder points downwards instead of upwards. Considering the extreme values, again top left to bottom right, are 50.45 compared to 33.48, 0, and 50.45, for minimum values; and 62.4 compared to 66.78, 72.08, and 62.4 for maximum values. The l_1 , l_2 , and l_∞ error norms for SL, ASD, and HEL are, 4.0×10^{-2} , 7.4×10^{-2} , and 3.5×10^{-1} ; and 1.6×10^{-1} , 3.1×10^{-1} , and 10×10^{-1} ; and 3.9×10^{-8} , 2.8×10^{-6} , and 1.6×10^{-4} , respectively.

4.2 Ranking

Ranking is performed by calculating error measures for each tracer and assigning points relative to their results. In the tables below, the 12 tested methods have been ranked based on calculation of the error norms, l_1 , l_2 , and l_∞ . To achieve the ranks given in the tables, the three error measures were calculated for each of the 58 chemical species and every method. For every error measure and for every species, the best

The HEL scheme tested with Chemistry

A. B. Hansen et al.

Title Page

Abstract

Introduction

Conclusions

References

Tables

Figures

◀

▶

◀

▶

Back

Close

Full Screen / Esc

Printer-friendly Version

Interactive Discussion



performing method was given the value 1, the second best, the value 2 and so on up to the worst performing method, which was given the value 12. For every method and for every error measure the mean value was calculated and given in the tables.

Error norms for the individual schemes and species are also given in the discussions of the various plots above. Tables 1–6 show results for the individual test cases and chemical regimes (rural and urban conditions), whereas the last table, Table 7, shows an overall ranking of all schemes and test cases.

Table 1 shows the ranking of the performance of the three schemes and their various temporal and spatial resolutions in regard to pure advection of the rotating cone. As a confirmation of the results above, the HEL scheme outperforms the two other schemes for all resolutions, the individual rankings of the HEL scheme show that the finer resolution the better, both spatially and temporally. Following the HEL scheme is ASD, finest resolution first, and last are the SL schemes. For SL, the individual rankings show that the finer spatial resolution and the higher Courant number, the better.

In Table 2 ranking for pure advection of the slotted cylinder is presented. The results are similar to those above with regard to ranking of the schemes, however, with regard to resolution the combination of coarser spatial resolution and higher Courant number seems to perform better for ASD (same overall rank). For HEL however, the combination of lowest Courant number and lowest temporal resolution performs best.

When considering rural chemistry and the rotating cone, see Table 3, the results are almost the same as for the rotating cone without chemistry, the only difference is for HEL, where the resolution with the highest Courant number performs better than the scheme with the second highest Courant number for rank of the l_1 and l_2 error norms. The difference between the overall ranks for the two resolutions is, however, small. Considering the individual values of l_1 and l_2 for O_3 and NO_2 , it is seen that resolution 3.1 gives the best results for NO_2 as expected, however, 10.1 gives the best score for O_3 .

Table 4 considers the slotted cylinder in a rural chemical regime, for HEL the individual ranking of the various resolutions is similar to that of the test for the slotted cylinder

The HEL scheme tested with Chemistry

A. B. Hansen et al.

Title Page

Abstract

Introduction

Conclusions

References

Tables

Figures



Back

Close

Full Screen / Esc

Printer-friendly Version

Interactive Discussion



with no chemistry. For ASD the order is the same as above, finest resolution first, and for SL the finer spatial resolution with the highest Courant number performs best.

Results for the most challenging chemical condition, urban chemistry, and the rotating cone are given in Table 5, again HEL outperforms all other schemes, with the same individual performance as for pure advection of the rotating cone. However, for SL and ASD the results differ from the above; SL with finest resolution and highest Courant number outperforms ASD for both resolutions, and even the SL schemes with finest spatial and temporal resolution and the one with highest Courant number outperforms ASD with the standard setup.

Table 6 presents results for the most challenging of the rotation tests, the slotted cylinder combined with urban chemistry. The best performing schemes are HEL with same individual ranking as for the previous tests for the slotted cylinder. This time, however, SL outperforms ASD for all resolutions, with the same individual order as for pure advection of the slotted cylinder. For ASD the finer temporal and spatial resolution scores better than the coarser resolution.

In general, when considering error norms for the species O_3 and NO_2 , not shown, the l_∞ values are, for each specific test, very close to if not identical for all resolutions. The difference lies in the l_1 and l_2 error norms, which are, compared to the values for the SL and ASD schemes, still fairly similar.

The final table, Table 7, ranks all the previous results to one overall rank of the schemes and various resolutions. The best performing scheme, for all resolutions, is HEL, with regard to the individual resolutions, the ranking is as for the tests of the rotating cone, for pure advection and with urban chemistry. Following HEL is ASD with the finest resolution, SL with finest spatial resolution and coarse temporal resolution, and ASD with coarse resolution. The remaining four SL schemes are first, the finest spatial and temporal resolution, and then for the coarse spatial resolution with highest Courant numbers first.

The HEL scheme tested with Chemistry

A. B. Hansen et al.

Title Page

Abstract

Introduction

Conclusions

References

Tables

Figures

⏪

⏩

◀

▶

Back

Close

Full Screen / Esc

Printer-friendly Version

Interactive Discussion



4.3 Dynamics

In this section tests have been performed where the HEL scheme has been used for solving the height/continuity equations in a channel type shallow water model, where dynamically passive tracers, with or without chemistry, are advected in a developing non-linear divergent flow. The shallow water model equations and the general model design is described in detail in Kaas (2008) for the locally mass conserving semi-Lagrangian (LMCSL) scheme, while required updates for the HEL scheme can be found in Kaas et al. (2012). The results obtained with HEL both with and without chemistry are here compared qualitatively with corresponding numbers obtained with LMCSL.

The grid distance is 156 km, and the time step 30 min, corresponding to a maximum Courant number of about 0.8. The initial surface height field and the bottom topography are shown in Fig. 10. The corresponding velocity field is simply initialized to be in geostrophic balance. The basic spatial shape of initial conditions for the tracers are shown in Fig. 11. This is simply a step function and a cosine hill of the same amplitude as the height of the step. In the tests where chemistry is applied all species are initialized with varying relative concentrations as in the rotation tests above.

The following figures present on the left side the surface height, i.e. the height of the fluid, and on the right side the final mixing ratios for the chemical species O_3 . LMCSL results are shown at the top, HEL without any mixing in the middle, and HEL with its standard mixing between Lagrangian parcels at the bottom.

Figure 12 presents results after 24 h simulation. The surface heights visually seem identical for the three cases after 24 h although the different numerical schemes are used. As can be seen the shapes of the square and the cosine hill, now visible in the O_3 mixing ratios, are distorted due to non-linearity of the velocity field. While the general pattern is similar for all schemes there are, however, also obvious differences. The LMCSL results in both the lowest and highest values, though not much higher than the max values for HEL with and without mixing, which are almost the same. The HEL

The HEL scheme tested with Chemistry

A. B. Hansen et al.

Title Page

Abstract

Introduction

Conclusions

References

Tables

Figures



Back

Close

Full Screen / Esc

Printer-friendly Version

Interactive Discussion



scheme, with or without mixing, does not generate the low concentrations that appear as undershoots in LMCSL around the deformed step function. The solution from the unmixed HEL show rather jagged edges of this “shape”, whereas the solution with mixing is more smooth around the edges. However, some overshoot wiggles are seen near the boundary of the “shape”. These are very important and are related to effect of the HEL mixing between very different concentrations in neighboring parcels.

When pure advection is considered the results are far smoother than for those simulations including chemistry. In Fig. 13 results are shown after 24 h simulation without chemistry. LMCSL generates both under and overshoots, whereas HEL perfectly reproduces the extreme values, both for the mixed and unmixed case. The edges of the concentrations are obviously smoother for the simulation with mixing, yet very similar.

After 480 h, as shown in Fig. 14, the overall trend is similar, but the results are clearly different. The minimum value for LMCSL is significantly lower than those for HEL, which are again similar, however, the maximum value for the unmixed HEL scheme is significantly higher than both the mixed HEL and LMCSL. In results from the mixed HEL (bottom plots) the field is much smoother than for the unmixed HEL, but not quite as smooth as the solution from LMCSL.

5 Conclusions

A newly developed transport scheme, the Hybrid Eulerian Lagrangian (HEL) scheme, has been combined with a module for atmospheric chemistry, and compared to two other traditional advection schemes: the pseudospectral scheme, referred to as the Eulerian Accurate Space Derivative (ASD) scheme, and a third order semi-Lagrangian (SL) scheme using a classical rotation test. The rotation tests have been designed to test and compare the advection schemes for different spatial and temporal resolutions in different chemical conditions (no chemistry, rural and urban) and for different shapes (cone and slotted cylinder) giving the advection schemes different challenges with respect to relatively slow or fast chemistry and smooth or sharp gradients, respectively.

The HEL scheme tested with Chemistry

A. B. Hansen et al.

Title Page

Abstract

Introduction

Conclusions

References

Tables

Figures



Back

Close

Full Screen / Esc

Printer-friendly Version

Interactive Discussion



**The HEL scheme
tested with
Chemistry**A. B. Hansen et al.

[Title Page](#)[Abstract](#)[Introduction](#)[Conclusions](#)[References](#)[Tables](#)[Figures](#)[Back](#)[Close](#)[Full Screen / Esc](#)[Printer-friendly Version](#)[Interactive Discussion](#)

In every test, error measures have been calculated and used for ranking of the advection schemes with respect to performance, i.e. lowest overall errors for all chemical species. Furthermore, to demonstrate the performance in deforming non-linear flow, HEL and a locally mass conserving semi Lagrangian (LMCSL) transport scheme have been tested in a shallow water model including transport of tracers.

The rotation results presented show that the new advection scheme, HEL, by far outperforms both the Eulerian and semi-Lagrangian schemes with very low error estimates compared to the two other schemes. For the rotating cone the results are similar to those for the slotted cylinder. However, when considering urban chemistry, for both the slotted cylinder and the rotating cone, ASD does not outperform SL in all cases.

The ranking shows that the HEL scheme in the tests with non-deforming flow and non-linear chemistry is superior to both the ASD and SL schemes, both for the individual test cases and for the general comparison. The HEL scheme scores the lowest (best) values in the ranking for all tests and for all error measures.

In the tests based on the shallow water model, the HEL scheme also performs better than the LMCSL scheme in the sense that positive definiteness/monotonicity is achieved for inert transport. The non-linear flow generated in the model results in completely unrealistic tracer distribution both with and without chemistry after some time unless a mixing between parcel concentrations is introduced. This occurs because neighboring parcels have followed different long term trajectories and therefore originates from very different locations. The degree of mixing is proportional to the instantaneous local deformation rate, and is therefore highly physically based. With this mixing a distribution of tracer concentrations become realistic, and more similar to that obtained with LMCSL, although it is slightly less diffusive and LMCSL.

In the dynamical tests emissions are not considered. A future aspect for the HEL scheme will be to implement emissions.

Acknowledgements. The present study is a part of the research of the Center for Energy, Environment and Health, financed by The Danish Strategic Research Program on Sustainable Energy under contract no 09-061417.

References

- Brandt, J., Silver, J. D., Frohn, L. M., Geels, C., Gross, A., Hansen, A. B., Hansen, K. M., Hedegaard, G. B., Skjøth, C. A., Villadsen, H., Zare, A., and Christensen, J. H.: An integrated model study for Europe and North America using the Danish Eulerian Hemispheric Model with focus on intercontinental transport of air pollution, *Atmos. Environ.*, 53, 156–176, 2012. 3701
- Crowley, W. P.: Numerical advection experiments, *Mon. Weather Rev.*, 96, 1–11, 1968. 3700
- Frohn, L. M., Christensen, J. H., and Brandt, J.: Development of a high resolution nested air pollution model: the numerical approach, *J. Comput. Phys.*, 179, 68–94, 2002. 3701
- Hansen, A. B., Brandt, J., Christensen, J. H., and Kaas, E.: Semi-Lagrangian methods in air pollution models, *Geosci. Model Dev.*, 4, 511–541, doi:10.5194/gmd-4-511-2011, 2011. 3700, 3701, 3702
- Kaas, E.: A simple and efficient locally mass conserving semi-Lagrangian transport scheme, *Tellus*, 60, 305–320, 2008. 3707
- Kaas, E., Sørensen, B., Lauritzen, P. H., and Hansen, A. B.: A hybrid Eulerian Lagrangian numerical scheme for solving prognostic equations in fluid dynamics, *J. Comput. Phys.*, submitted, 2012. 3697, 3700, 3707
- Lauritzen, P. H. and Thuburn, J.: Evaluating advection/transport schemes using interrelated tracers, scatter plots, and numerical diagnostics, *Q. J. Roy. Meteorol. Soc.*, 138, 906–918, 2012. 3697
- Machenhauer, B., Kaas, E., and Lauritzen, P. H.: *Handbook on Numerical Analysis – Finite Volume Methods in Meteorology*, Elsevier, 2008. 3697
- Molenkamp, C. R.: Accuracy of finite-difference methods applied to the advection equation, *J. Appl. Meteorol.*, 7, 160–167, 1968. 3700
- Rasch, P. J. and Williamson, D. L.: Computational aspects of moisture transport in global models of the atmosphere, *Q. J. Roy. Meteorol. Soc.*, 116, 1071–1090, 1990. 3697
- Reithmeier, C. and Sausen, R.: ATTILA: atmospheric tracer transport in a Lagrangian model, *Tellus*, 54B, 278–299, 2002. 3697
- Smagorinsky, J.: General circulation experiments with the primitive equations: I. The basic experiment, *Mon. Weather Rev.*, 91, 99–164, 1963. 3698
- Stenke, A., Grewe, V., and Ponater, M.: Lagrangian transport of water vapor and cloud water in the ECHAM4 GCM and its impact on the cold bias, *Clim. Dynam.*, 31, 491–506, 2008. 3697

The HEL scheme tested with Chemistry

A. B. Hansen et al.

[Title Page](#)

[Abstract](#)

[Introduction](#)

[Conclusions](#)

[References](#)

[Tables](#)

[Figures](#)

[⏪](#)

[⏩](#)

[◀](#)

[▶](#)

[Back](#)

[Close](#)

[Full Screen / Esc](#)

[Printer-friendly Version](#)

[Interactive Discussion](#)



Stenke, A., Dameris, M., Grewe, V., and Garny, H.: Implications of Lagrangian transport for simulations with a coupled chemistry-climate model, *Atmos. Chem. Phys.*, 9, 5489–5504, doi:10.5194/acp-9-5489-2009, 2009. 3697

5 Zerroukat, M., Wood, N., and Staniforth, A.: SLICE: a semi-Lagrangian inherently conserving and efficient scheme for transport problems, *Q. J. Roy. Meteorol. Soc.*, 128, 2801–2820, 2002. 3700

**The HEL scheme
tested with
Chemistry**

A. B. Hansen et al.

Title Page

Abstract

Introduction

Conclusions

References

Tables

Figures

◀

▶

◀

▶

Back

Close

Full Screen / Esc

Printer-friendly Version

Interactive Discussion



The HEL scheme tested with Chemistry

A. B. Hansen et al.

Table 1. Ranking results for the rotating cone with pure advection. Showing rank of the ranked error measures, rank of error measure l_1 , l_2 , and l_∞ followed by method, maximum Courant number, grid resolution, and time step.

| rank (all) | rank (l_1) | rank (l_2) | rank (l_∞) | Method | CFL _{max} | Δx | Δt |
|------------|----------------|----------------|---------------------|--------|--------------------|------------|------------|
| 1.54 | 1.42 | 1.42 | 1.79 | HEL | 0.327 | 0.5 | 45 |
| 2.60 | 2.33 | 2.33 | 3.12 | HEL | 0.654 | 0.5 | 90 |
| 2.81 | 2.67 | 2.67 | 3.08 | HEL | 0.327 | 1.0 | 90 |
| 3.81 | 3.96 | 3.96 | 3.50 | HEL | 0.981 | 1.0 | 270 |
| 4.25 | 4.62 | 4.62 | 3.50 | HEL | 3.27 | 1.0 | 900 |
| 6.01 | 6.00 | 6.00 | 6.04 | ASD | 0.327 | 0.5 | 45 |
| 6.99 | 7.00 | 7.00 | 6.96 | ASD | 0.327 | 1.0 | 90 |
| 8.01 | 8.00 | 8.00 | 8.04 | SL | 0.654 | 0.5 | 90 |
| 8.99 | 9.00 | 9.00 | 8.96 | SL | 0.327 | 0.5 | 45 |
| 10.00 | 10.00 | 10.00 | 10.00 | SL | 3.27 | 1.0 | 900 |
| 11.00 | 11.00 | 11.00 | 11.00 | SL | 0.981 | 1.0 | 270 |
| 12.00 | 12.00 | 12.00 | 12.00 | SL | 0.327 | 1.0 | 90 |

Title Page

Abstract

Introduction

Conclusions

References

Tables

Figures

◀

▶

◀

▶

Back

Close

Full Screen / Esc

Printer-friendly Version

Interactive Discussion



The HEL scheme tested with Chemistry

A. B. Hansen et al.

Table 2. Ranking results for the slotted cylinder with pure advection. Showing rank of the ranked error measures, rank of error measure l_1 , l_2 , and l_∞ followed by method, maximum Courant number, grid resolution, and time step.

| rank (all) | rank (l_1) | rank (l_2) | rank(l_∞) | Method | CFL _{max} | Δx | Δt |
|------------|----------------|----------------|--------------------|--------|--------------------|------------|------------|
| 1.51 | 1.17 | 1.17 | 2.21 | HEL | 0.327 | 0.5 | 45 |
| 2.40 | 2.75 | 2.25 | 2.21 | HEL | 0.327 | 1.0 | 90 |
| 2.79 | 2.33 | 2.83 | 3.21 | HEL | 0.654 | 0.5 | 90 |
| 3.71 | 3.92 | 3.92 | 3.29 | HEL | 0.981 | 1.0 | 270 |
| 4.58 | 4.83 | 4.83 | 4.08 | HEL | 3.27 | 1.0 | 900 |
| 6.67 | 6.00 | 6.00 | 8.00 | ASD | 0.327 | 0.5 | 45 |
| 6.67 | 7.00 | 7.00 | 6.00 | ASD | 0.327 | 1.0 | 90 |
| 9.00 | 10.00 | 10.00 | 7.00 | SL | 3.27 | 1.0 | 900 |
| 9.01 | 8.00 | 8.00 | 11.04 | SL | 0.654 | 0.5 | 90 |
| 9.99 | 9.00 | 9.00 | 11.96 | SL | 0.327 | 0.5 | 45 |
| 10.33 | 11.00 | 11.00 | 9.00 | SL | 0.981 | 1.0 | 270 |
| 11.33 | 12.00 | 12.00 | 10.00 | SL | 0.327 | 1.0 | 90 |

Title Page

Abstract

Introduction

Conclusions

References

Tables

Figures

⏪

⏩

◀

▶

Back

Close

Full Screen / Esc

Printer-friendly Version

Interactive Discussion



The HEL scheme tested with Chemistry

A. B. Hansen et al.

Table 3. Ranking results for the rotating cone with rural chemistry. Showing rank of the ranked error measures, rank of error measure l_1 , l_2 , and l_∞ followed by method, maximum Courant number, grid resolution, and time step.

| rank (all) | rank (l_1) | rank (l_2) | rank (l_∞) | Method | CFL _{max} | Δx | Δt |
|------------|----------------|----------------|---------------------|--------|--------------------|------------|------------|
| 1.98 | 1.62 | 1.99 | 2.34 | HEL | 0.327 | 0.5 | 45 |
| 2.63 | 2.23 | 2.54 | 3.12 | HEL | 0.654 | 0.5 | 90 |
| 2.91 | 3.08 | 3.06 | 2.58 | HEL | 0.327 | 1.0 | 90 |
| 3.62 | 3.88 | 3.61 | 3.36 | HEL | 3.27 | 1.0 | 900 |
| 3.94 | 4.19 | 4.03 | 3.59 | HEL | 0.981 | 1.0 | 270 |
| 6.00 | 6.00 | 5.99 | 6.00 | ASD | 0.327 | 0.5 | 45 |
| 7.00 | 7.02 | 6.97 | 7.00 | ASD | 0.327 | 1.0 | 90 |
| 8.04 | 8.06 | 8.01 | 8.06 | SL | 0.654 | 0.5 | 90 |
| 8.96 | 8.98 | 8.92 | 8.98 | SL | 0.327 | 0.5 | 45 |
| 10.00 | 10.02 | 9.95 | 10.02 | SL | 3.27 | 1.0 | 900 |
| 11.01 | 11.00 | 11.00 | 11.02 | SL | 0.981 | 1.0 | 270 |
| 11.93 | 11.93 | 11.93 | 11.93 | SL | 0.327 | 1.0 | 90 |

Title Page

Abstract

Introduction

Conclusions

References

Tables

Figures



Back

Close

Full Screen / Esc

Printer-friendly Version

Interactive Discussion



The HEL scheme tested with Chemistry

A. B. Hansen et al.

Table 4. Ranking results for the slotted cylinder with rural chemistry. Showing rank of the ranked error measures, rank of error measure l_1 , l_2 , and l_∞ followed by method, maximum Courant number, grid resolution, and time step.

| rank (all) | rank (l_1) | rank (l_2) | rank (l_∞) | Method | CFL _{max} | Δx | Δt |
|------------|----------------|----------------|---------------------|--------|--------------------|------------|------------|
| 1.76 | 1.50 | 1.54 | 2.23 | HEL | 0.327 | 0.5 | 45 |
| 2.62 | 2.94 | 2.47 | 2.46 | HEL | 0.327 | 1.0 | 90 |
| 2.73 | 2.14 | 2.77 | 3.28 | HEL | 0.654 | 0.5 | 90 |
| 3.75 | 3.98 | 3.94 | 3.32 | HEL | 0.981 | 1.0 | 270 |
| 4.14 | 4.44 | 4.28 | 3.70 | HEL | 3.27 | 1.0 | 900 |
| 6.44 | 6.15 | 6.02 | 7.17 | ASD | 0.327 | 0.5 | 45 |
| 7.11 | 7.78 | 7.17 | 6.39 | ASD | 0.327 | 1.0 | 90 |
| 8.83 | 7.91 | 8.28 | 10.31 | SL | 0.654 | 0.5 | 90 |
| 9.18 | 9.67 | 9.83 | 8.04 | SL | 3.27 | 1.0 | 900 |
| 9.83 | 8.80 | 9.06 | 11.65 | SL | 0.327 | 0.5 | 45 |
| 10.30 | 10.89 | 10.89 | 9.13 | SL | 0.981 | 1.0 | 270 |
| 11.30 | 11.81 | 11.76 | 10.32 | SL | 0.327 | 1.0 | 90 |

Title Page

Abstract

Introduction

Conclusions

References

Tables

Figures

⏪

⏩

◀

▶

Back

Close

Full Screen / Esc

Printer-friendly Version

Interactive Discussion



The HEL scheme tested with Chemistry

A. B. Hansen et al.

Table 5. Ranking results for the rotating cone with urban chemistry. Showing rank of the ranked error measures, rank of error measure l_1 , l_2 , and l_∞ followed by method, maximum Courant number, grid resolution, and time step.

| rank (all) | rank (l_1) | rank (l_2) | rank (l_∞) | Method | CFL _{max} | Δx | Δt |
|------------|----------------|----------------|---------------------|--------|--------------------|------------|------------|
| 2.04 | 1.57 | 2.00 | 2.55 | HEL | 0.327 | 0.5 | 45 |
| 2.33 | 1.97 | 2.23 | 2.80 | HEL | 0.654 | 0.5 | 90 |
| 3.02 | 3.10 | 3.14 | 2.81 | HEL | 0.327 | 1.0 | 90 |
| 3.78 | 4.13 | 3.89 | 3.31 | HEL | 0.981 | 1.0 | 270 |
| 3.86 | 4.22 | 3.83 | 3.54 | HEL | 3.27 | 1.0 | 900 |
| 6.86 | 6.67 | 6.78 | 7.13 | SL | 0.654 | 0.5 | 90 |
| 7.31 | 7.33 | 7.33 | 7.28 | ASD | 0.327 | 0.5 | 45 |
| 7.98 | 7.76 | 7.94 | 8.22 | SL | 0.327 | 0.5 | 45 |
| 8.91 | 8.94 | 8.94 | 8.83 | SL | 3.27 | 1.0 | 900 |
| 9.91 | 10.31 | 9.81 | 9.59 | ASD | 0.327 | 1.0 | 90 |
| 10.47 | 10.48 | 10.52 | 10.41 | SL | 0.981 | 1.0 | 270 |
| 11.54 | 11.50 | 11.57 | 11.54 | SL | 0.327 | 1.0 | 90 |

Title Page

Abstract

Introduction

Conclusions

References

Tables

Figures

◀

▶

◀

▶

Back

Close

Full Screen / Esc

Printer-friendly Version

Interactive Discussion



The HEL scheme tested with Chemistry

A. B. Hansen et al.

Table 6. Ranking results for the slotted cylinder with urban chemistry. Showing rank of the ranked error measures, rank of error measure l_1 , l_2 , and l_∞ followed by method, maximum Courant number, grid resolution, and time step.

| rank (all) | rank (l_1) | rank (l_2) | rank (l_∞) | Method | CFL _{max} | Δx | Δt |
|------------|----------------|----------------|---------------------|--------|--------------------|------------|------------|
| 1.94 | 1.74 | 1.89 | 2.20 | HEL | 0.327 | 0.5 | 45 |
| 2.67 | 2.98 | 2.61 | 2.43 | HEL | 0.327 | 1.0 | 90 |
| 2.75 | 2.22 | 2.69 | 3.35 | HEL | 0.654 | 0.5 | 90 |
| 3.55 | 3.65 | 3.60 | 3.41 | HEL | 0.981 | 1.0 | 270 |
| 4.08 | 4.41 | 4.21 | 3.61 | HEL | 3.27 | 1.0 | 900 |
| 7.16 | 7.43 | 7.28 | 6.78 | SL | 3.27 | 1.0 | 900 |
| 7.29 | 6.67 | 6.83 | 8.38 | SL | 0.654 | 0.5 | 90 |
| 8.15 | 7.59 | 7.69 | 9.17 | SL | 0.327 | 0.5 | 45 |
| 8.67 | 9.24 | 9.19 | 7.57 | SL | 0.981 | 1.0 | 270 |
| 9.79 | 10.15 | 10.15 | 9.06 | SL | 0.327 | 1.0 | 90 |
| 10.79 | 10.50 | 10.56 | 11.31 | ASD | 0.327 | 0.5 | 45 |
| 11.15 | 11.43 | 11.31 | 10.72 | ASD | 0.327 | 1.0 | 90 |

Title Page

Abstract

Introduction

Conclusions

References

Tables

Figures



Back

Close

Full Screen / Esc

Printer-friendly Version

Interactive Discussion



The HEL scheme tested with Chemistry

A. B. Hansen et al.

Title Page

Abstract

Introduction

Conclusions

References

Tables

Figures



Back

Close

Full Screen / Esc

Printer-friendly Version

Interactive Discussion



Table 7. Ranking results for the sum of rank(all) from all six ranking tables. Showing the sum of the total rank, rank(rank(all)), method, maximum courant number, grid size, and time step.

| rank (rank(all)) | Method | CFL _{max} | Δx | Δt |
|------------------|--------|--------------------|------------|------------|
| 10.77 | HEL | 0.327 | 0.5 | 45 |
| 15.83 | HEL | 0.654 | 0.5 | 90 |
| 16.43 | HEL | 0.327 | 1.0 | 90 |
| 22.51 | HEL | 0.981 | 1.0 | 270 |
| 24.53 | HEL | 3.27 | 1.0 | 900 |
| 43.22 | ASD | 0.327 | 0.5 | 45 |
| 48.04 | SL | 0.654 | 0.5 | 90 |
| 48.83 | ASD | 0.327 | 1.0 | 90 |
| 53.90 | SL | 0.327 | 0.5 | 45 |
| 54.25 | SL | 3.27 | 1.0 | 900 |
| 61.78 | SL | 0.981 | 1.0 | 270 |
| 67.89 | SL | 0.327 | 1.0 | 90 |

**The HEL scheme
tested with
Chemistry**A. B. Hansen et al.

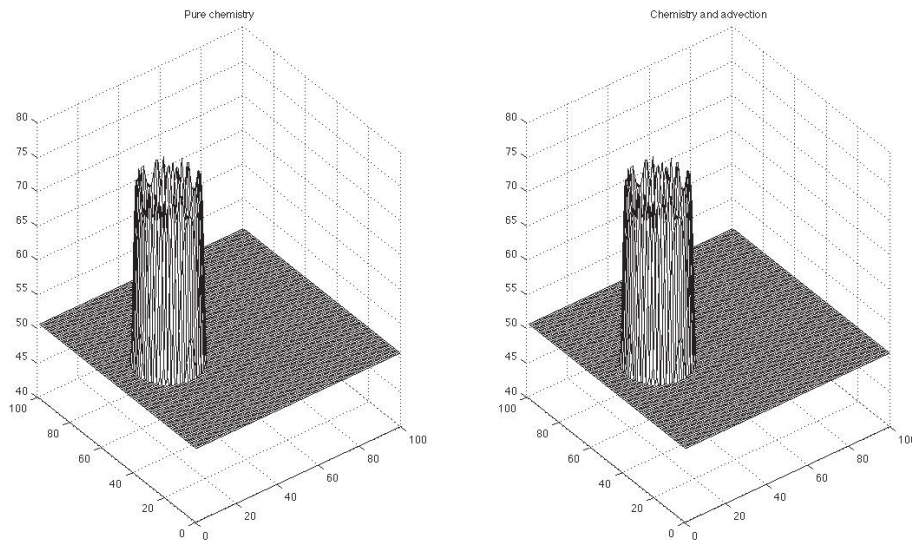


Fig. 1. HEL using urban chemistry O₃ rotating cone standard resolution. Rotation test for HEL using the rotating cone for O₃ with urban conditions and resolution 1_1, with $\Delta t = 90$ s, $\Delta x = 1.0$, and $C = 0.327$. The results are given for pure chemistry (left) and combined chemistry and advection (right). The minimum and maximum values for the respective plots are: Left: minimum = 50.45, maximum = 77.47. Right: minimum = 50.45, maximum = 77.47.

[Title Page](#)[Abstract](#)[Introduction](#)[Conclusions](#)[References](#)[Tables](#)[Figures](#)[⏪](#)[⏩](#)[◀](#)[▶](#)[Back](#)[Close](#)[Full Screen / Esc](#)[Printer-friendly Version](#)[Interactive Discussion](#)

The HEL scheme tested with ChemistryA. B. Hansen et al.

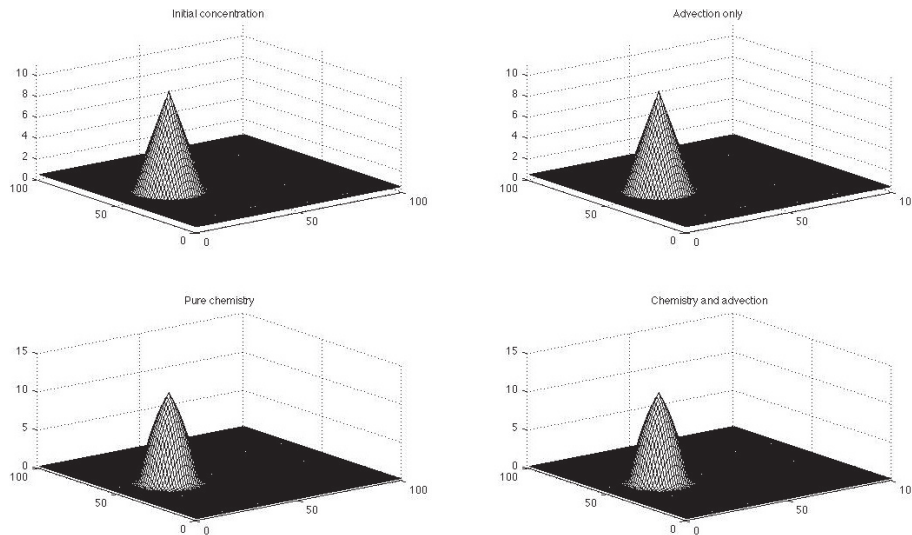


Fig. 2. HEL using urban chemistry NO_2 rotating cone standard resolution. Rotation test for HEL using the rotating cone for NO_2 with urban conditions and resolution 1_1, with $\Delta t = 90$ s, $\Delta x = 1.0$, and $C = 0.327$. The results are given for the initial condition (top left) and model runs with pure advection (top right), pure chemistry (bottom left), and combined chemistry and advection (bottom right). The minimum and maximum values for the respective plots are: Top left: min = 0.5000, max = 10.000. Top right: min = 0.5000, max = 10.0000. Bottom left: min = 0.1369, max = 11.8000. Bottom right: min = 0.1369, max = 11.8000.

[Title Page](#)[Abstract](#)[Introduction](#)[Conclusions](#)[References](#)[Tables](#)[Figures](#)[⏪](#)[⏩](#)[◀](#)[▶](#)[Back](#)[Close](#)[Full Screen / Esc](#)[Printer-friendly Version](#)[Interactive Discussion](#)

**The HEL scheme
tested with
Chemistry**A. B. Hansen et al.

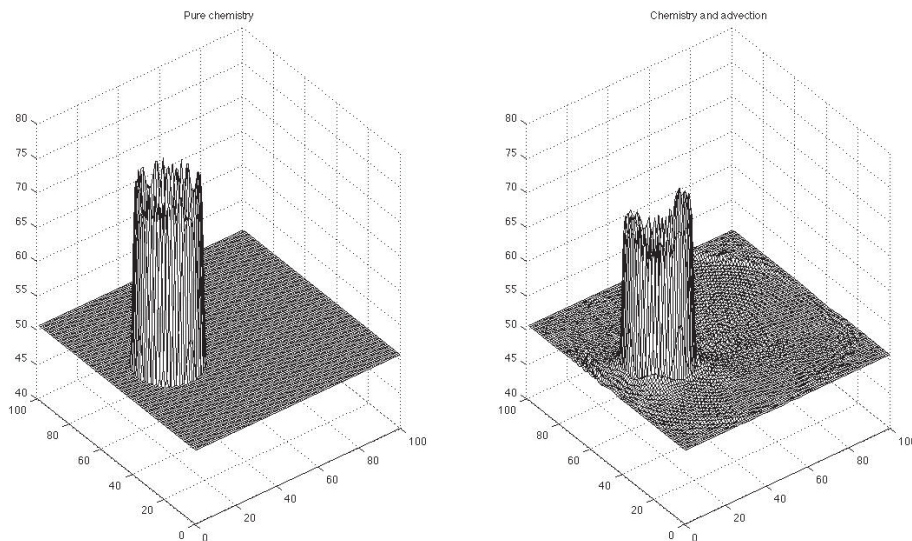


Fig. 3. ASD using urban chemistry O₃ rotating cone standard resolution. Rotation test for ASD using the rotating cone for O₃ with urban conditions and resolution 1_1, with $\Delta t = 90$ s, $\Delta x = 1.0$, and $C = 0.327$. The results are given for pure chemistry (left) and combined chemistry and advection (right). The minimum and maximum values for the respective plots are: Left: minimum = 50.45, maximum = 77.47. Right: minimum = 49.21, maximum = 74.22.

[Title Page](#)[Abstract](#)[Introduction](#)[Conclusions](#)[References](#)[Tables](#)[Figures](#)[⏪](#)[⏩](#)[◀](#)[▶](#)[Back](#)[Close](#)[Full Screen / Esc](#)[Printer-friendly Version](#)[Interactive Discussion](#)

The HEL scheme tested with ChemistryA. B. Hansen et al.

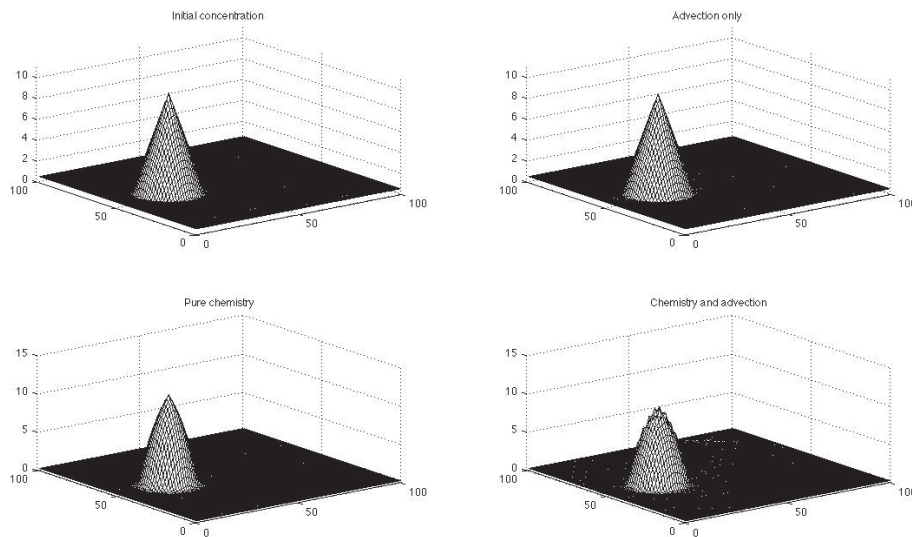


Fig. 4. ASD using urban chemistry NO_2 rotating cone standard resolution. Rotation test for ASD using the rotating cone for NO_2 with urban conditions and resolution 1_1, with $\Delta t = 90$ s, $\Delta x = 1.0$, and $C = 0.327$. The results are given for the initial condition (top left) and model runs with pure advection (top right), pure chemistry (bottom left), and combined chemistry and advection (bottom right). The minimum and maximum values for the respective plots are: Top left: min = 0.5000, max = 10.0000. Top right: min = 0.4615, max = 9.8540. Bottom left: min = 0.1369, max = 11.8000. Bottom right: min = 0.0633, max = 10.2900.

[Title Page](#)[Abstract](#)[Introduction](#)[Conclusions](#)[References](#)[Tables](#)[Figures](#)[⏪](#)[⏩](#)[◀](#)[▶](#)[Back](#)[Close](#)[Full Screen / Esc](#)[Printer-friendly Version](#)[Interactive Discussion](#)

**The HEL scheme
tested with
Chemistry**

A. B. Hansen et al.

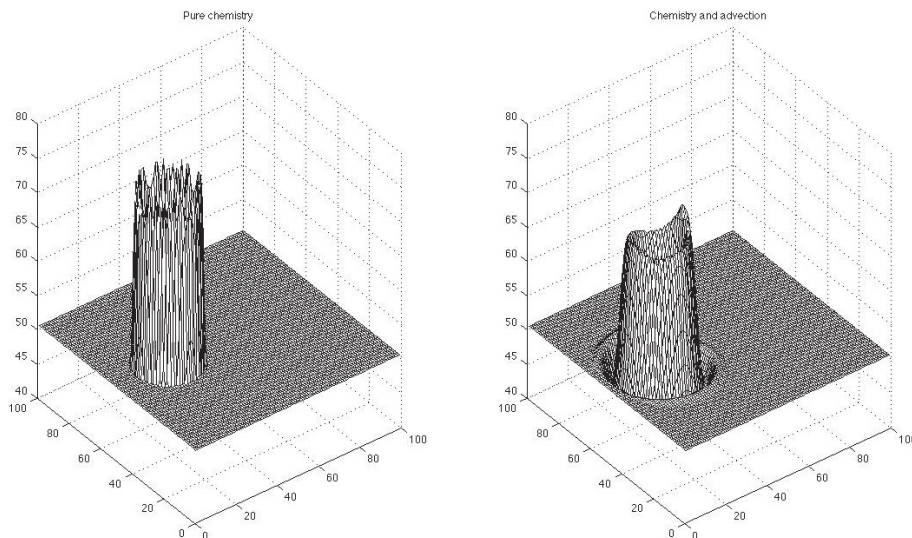


Fig. 5. SL using urban chemistry O_3 rotating cone standard resolution. Rotation test for SL using the rotating cone for O_3 with urban conditions and resolution 1_1, with $\Delta t = 90$ s, $\Delta x = 1.0$, and $C = 0.327$. The results are given for pure chemistry (left) and combined chemistry and advection (right). The minimum and maximum values for the respective plots are: Left: minimum = 50.45, maximum = 77.47. Right: minimum = 46.22, maximum = 71.86.

[Title Page](#)[Abstract](#)[Introduction](#)[Conclusions](#)[References](#)[Tables](#)[Figures](#)[⏪](#)[⏩](#)[◀](#)[▶](#)[Back](#)[Close](#)[Full Screen / Esc](#)[Printer-friendly Version](#)[Interactive Discussion](#)

**The HEL scheme
tested with
Chemistry**A. B. Hansen et al.

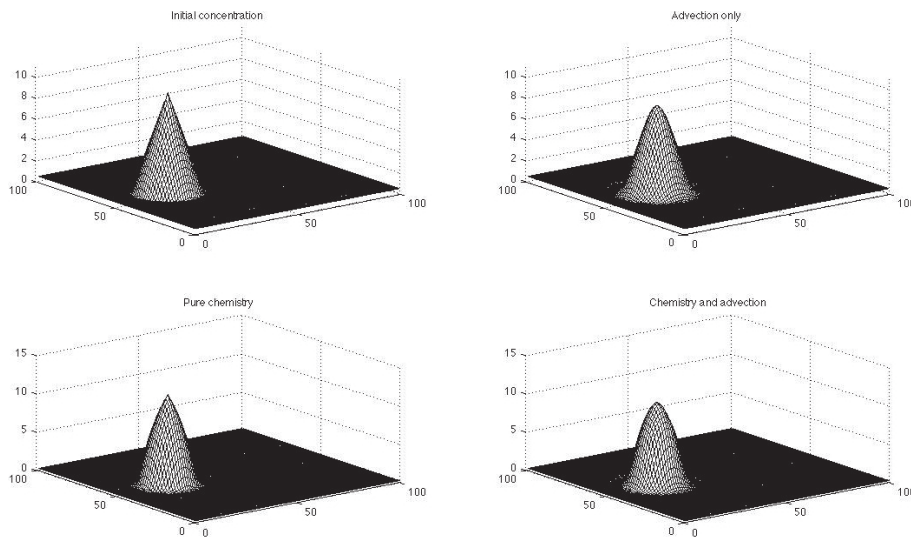


Fig. 6. SL using urban chemistry NO_2 rotating cone standard resolution. Rotation test for SL using the rotating cone for NO_2 with urban conditions and resolution 1_1, with $\Delta t = 90$ s, $\Delta x = 1.0$, and $C = 0.327$. The results are given for the initial condition (top left) and model runs with pure advection (top right), pure chemistry (bottom left), and combined chemistry and advection (bottom right). The minimum and maximum values for the respective plots are: Top left: min = 0.5000, max = 10.0000. Top right: min = 0.4029, max = 8.7530. Bottom left: min = 0.1369, max = 11.8000. Bottom right: min = 0.0429, max = 10.7500.

[Title Page](#)[Abstract](#)[Introduction](#)[Conclusions](#)[References](#)[Tables](#)[Figures](#)[⏪](#)[⏩](#)[◀](#)[▶](#)[Back](#)[Close](#)[Full Screen / Esc](#)[Printer-friendly Version](#)[Interactive Discussion](#)

The HEL scheme tested with Chemistry

A. B. Hansen et al.

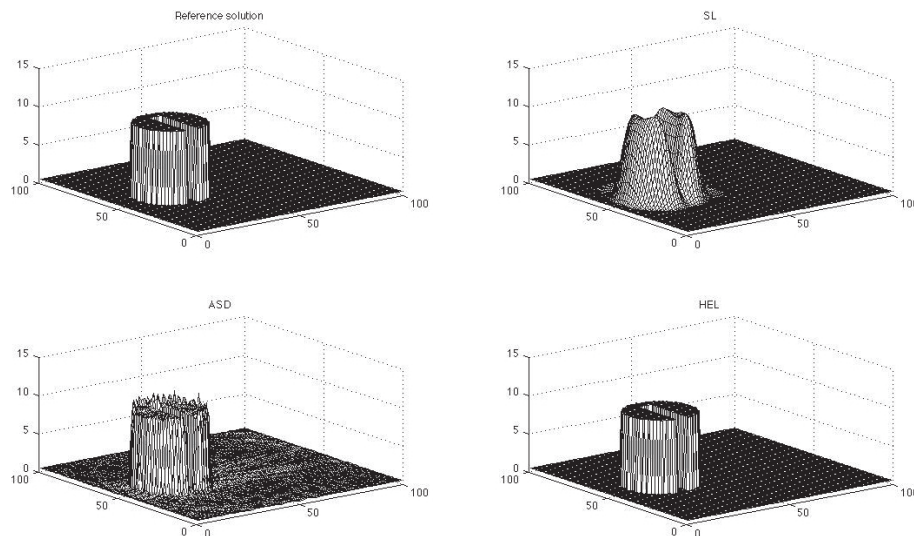


Fig. 7. Slotted cylinder, pure advection, $\Delta t = 90\text{s}$, $\Delta x = 1.0$, $C = 0.327$. Rotation test with the slotted cylinder for pure advection and resolution 1_1, with $\Delta t = 90\text{s}$, $\Delta x = 1.0$, and $C = 0.327$. The results are given for initial concentration (top left) and pure advection using for SL (top right), ASD (bottom left), and HEL (bottom right). The minimum and maximum values for the respective plots are: Top left: min = 0.5000, max = 10.0000. Top right: min = -0.0676, max = 11.3900. Bottom left: min = -0.7790, max = 11.6400. Bottom right: min = 0.5000, max = 10.0000.

Title Page

Abstract

Introduction

Conclusions

References

Tables

Figures



Back

Close

Full Screen / Esc

Printer-friendly Version

Interactive Discussion



The HEL scheme tested with Chemistry

A. B. Hansen et al.

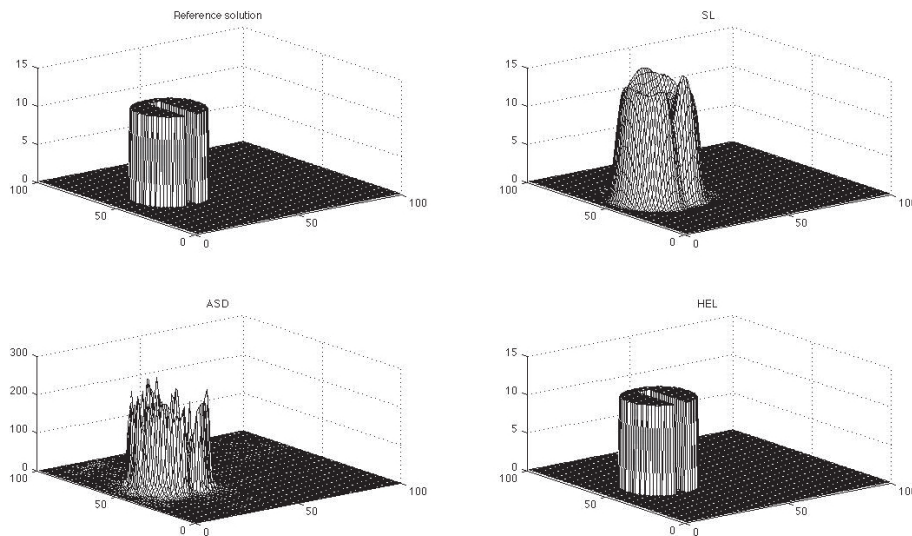


Fig. 8. Slotted cylinder, NO_2 , $\Delta t = 90\text{ s}$, $\Delta x = 1.0$, $C = 0.327$. Rotation test with the slotted cylinder for NO_2 using urban chemistry and resolution 1_1, with $\Delta t = 90\text{ s}$, $\Delta x = 1.0$, and $C = 0.327$. The results are given for pure chemistry (top left) and chemistry and advection for SL (top right), ASD (bottom left), and HEL (bottom right). The minimum and maximum values for the respective plots are: Top left: min = 0.1369, max = 11.8000. Top right: min = 0, max = 16.4200. Bottom left: min = 0, max = 269,2000. Bottom right: min = 0.1369, max = 11.8000. Note, the vertical axis on the bottom left plot is the interval 0–300, whereas the other are in the interval 0–15.

Title Page

Abstract

Introduction

Conclusions

References

Tables

Figures

◀

▶

◀

▶

Back

Close

Full Screen / Esc

Printer-friendly Version

Interactive Discussion



The HEL scheme tested with Chemistry

A. B. Hansen et al.

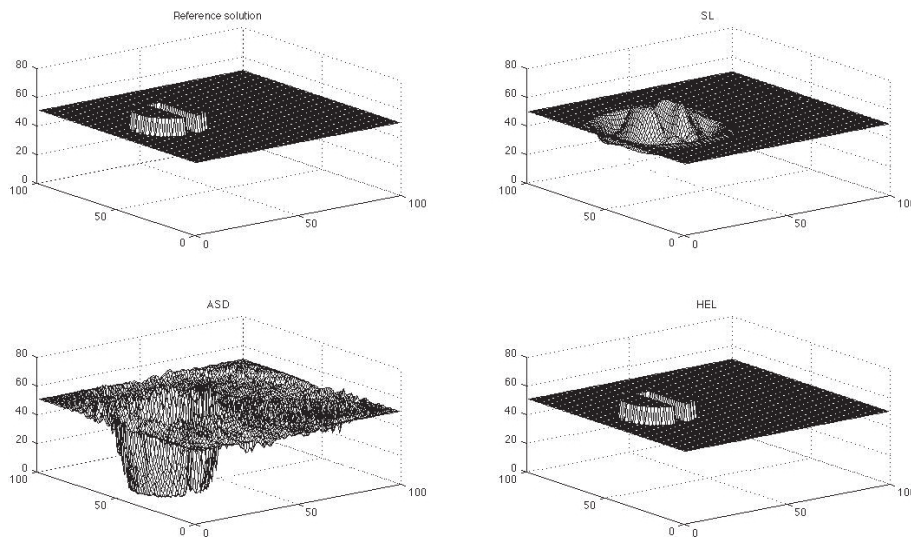


Fig. 9. Slotted cylinder, O_3 , $\Delta t = 90\text{ s}$, $\Delta x = 1.0$, $C = 0.327$. Rotation test with the slotted cylinder for O_3 for advection and chemistry combined for urban chemistry conditions and resolution 1_1, with $\Delta t = 90\text{ s}$, $\Delta x = 1.0$, and $C = 0.327$. The results are given for pure chemistry (top left) and chemistry and advection for SL (top right), ASD (bottom left), and HEL (bottom right). The minimum and maximum values for the respective plots are: Top left: min = 50.45, max = 62.40. Top right: min = 33.48, max = 66.78. Bottom left: min = 0, max = 72.08. Bottom right: min = 50.45, max = 62.40.

Title Page

Abstract

Introduction

Conclusions

References

Tables

Figures

⏪

⏩

◀

▶

Back

Close

Full Screen / Esc

Printer-friendly Version

Interactive Discussion



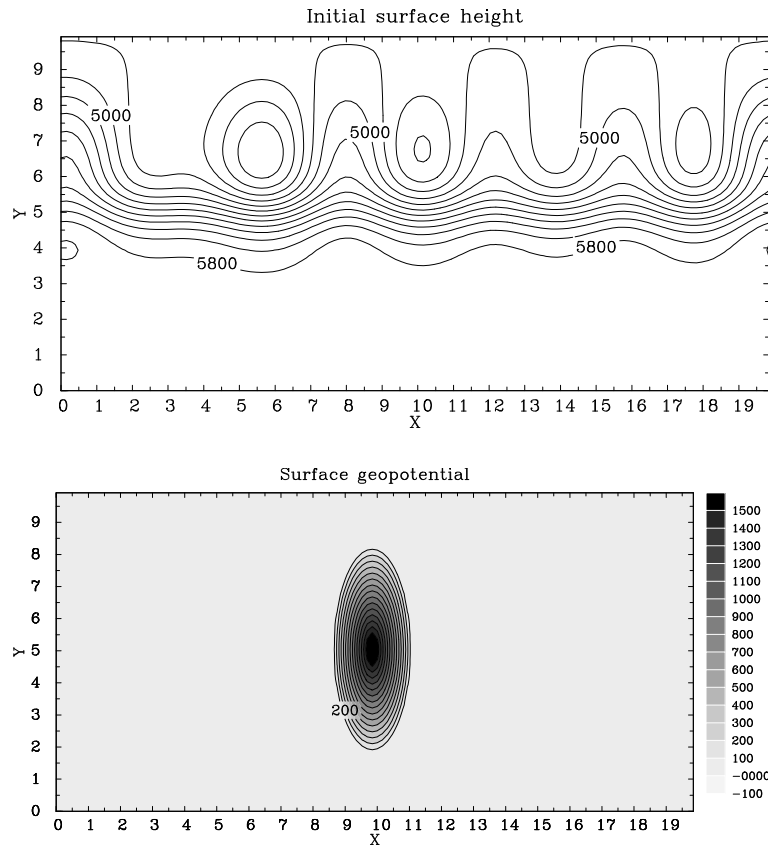


Fig. 10. Upper panel: initial surface height of the general fluid in the shallow water model. Lower panel: surface geopotential height, i.e. the initial thickness of the fluid is equal to the values in the left minus the right plots.

The HEL scheme tested with Chemistry

A. B. Hansen et al.

Title Page

Abstract

Introduction

Conclusions

References

Tables

Figures

◀

▶

◀

▶

Back

Close

Full Screen / Esc

Printer-friendly Version

Interactive Discussion



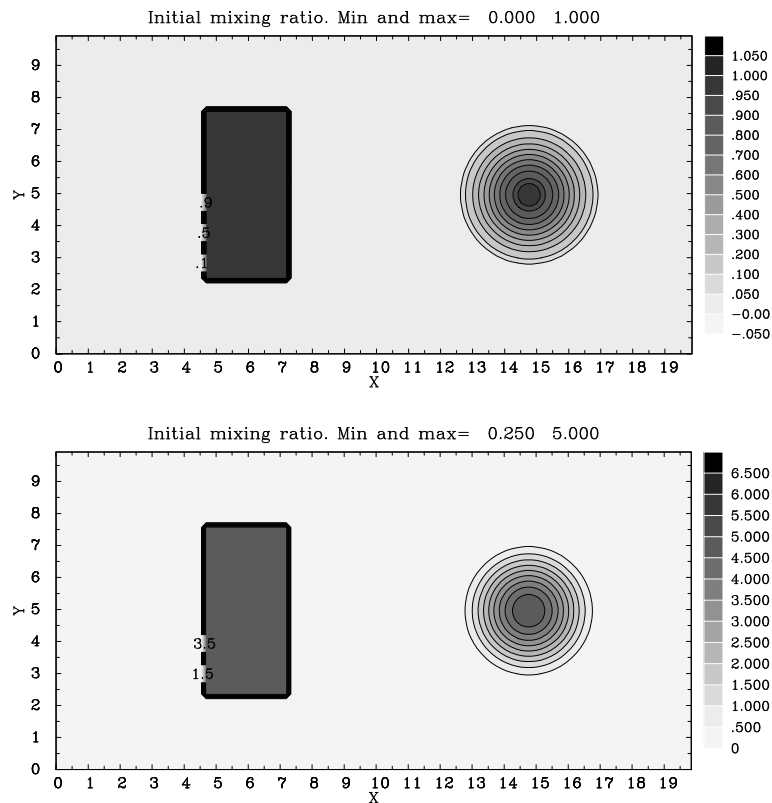


Fig. 11. Upper panel: initial concentration for an inert tracer. Lower panel: corresponding initial tracer concentration for the chemical species NO_2 in units of ppbv (parts per billion by volume) as it is used in the simulations with active urban chemistry.

The HEL scheme tested with Chemistry

A. B. Hansen et al.

Title Page

Abstract Introduction

Conclusions References

Tables Figures

◀ ▶

◀ ▶

Back Close

Full Screen / Esc

Printer-friendly Version

Interactive Discussion



The HEL scheme
tested with
Chemistry

A. B. Hansen et al.

Title Page

Abstract

Introduction

Conclusions

References

Tables

Figures

◀

▶

◀

▶

Back

Close

Full Screen / Esc

Printer-friendly Version

Interactive Discussion

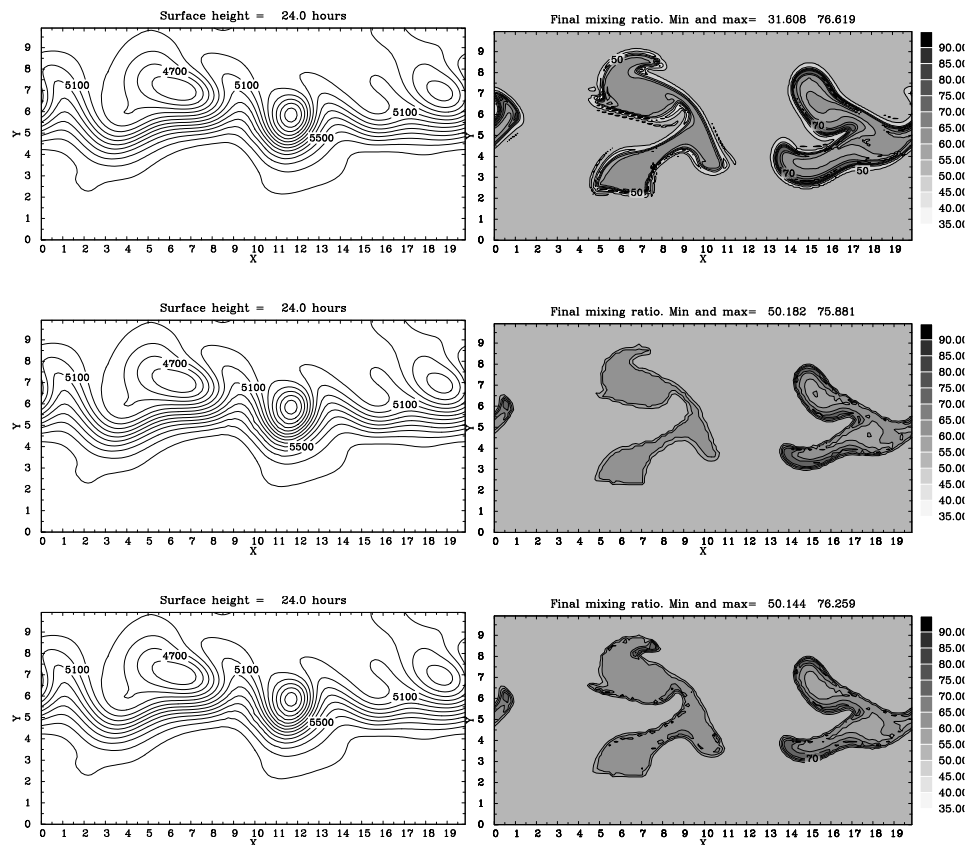


Fig. 12. Surface height (left) and concentration fields for O₃ in units of ppbv (right) after 24 h simulation for LMCSL (top), HEL without mixing (middle), and HEL with mixing (bottom).

**The HEL scheme
tested with
Chemistry**

A. B. Hansen et al.

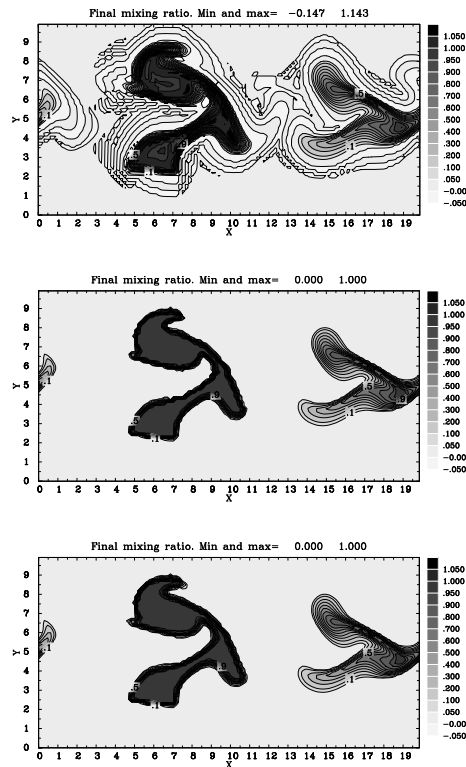


Fig. 13. Mixing ratio for the inert tracer after 24 h of simulation for pure advection without chemistry for LMCSL (top), HEL without mixing (middle), and HEL with mixing (bottom).

The HEL scheme tested with Chemistry

A. B. Hansen et al.

Title Page

Abstract

Introduction

Conclusions

References

Tables

Figures



Back

Close

Full Screen / Esc

Printer-friendly Version

Interactive Discussion

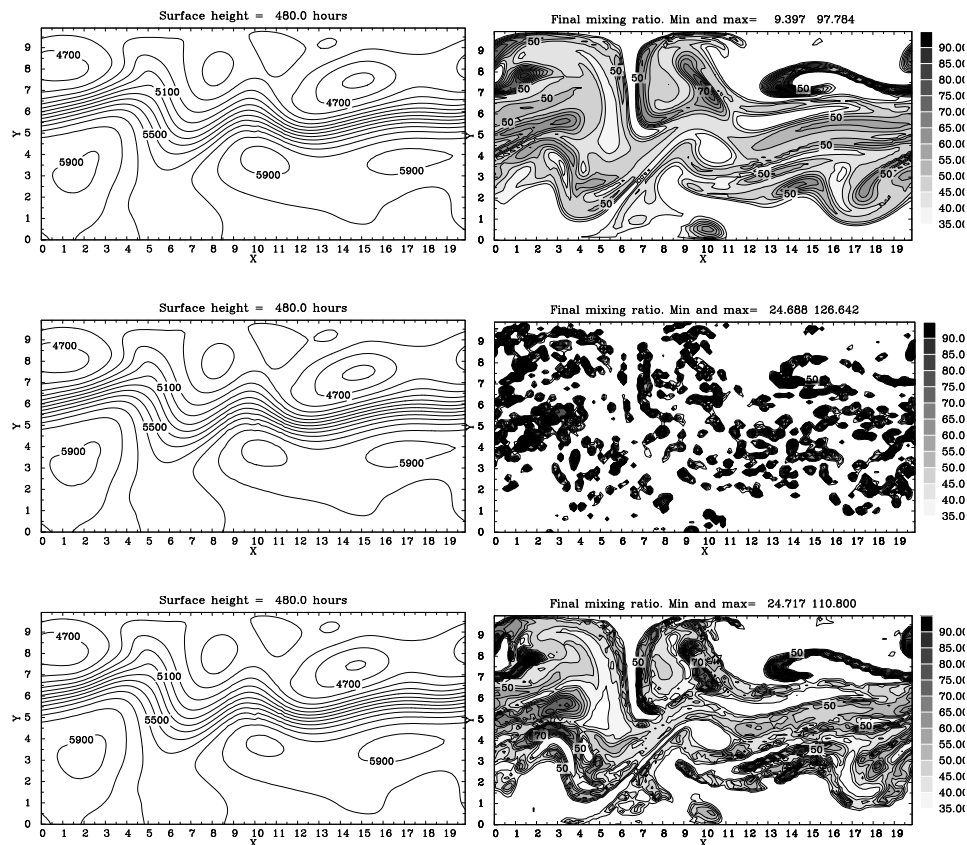


Fig. 14. Surface height (left) and concentration of O_3 (right, unit ppbv) after 480 h of simulation for LMCSL (top), HEL without mixing (middle), and HEL with mixing (bottom).